Unique Temperature-Dependent Supramolecular Self-Assembly: From Hierarchical 1D Nanostructures to Super Hydrogel

Yan Qiao, Yiyang Lin, Zhiyi Yang, Huanfa Chen, Shaofei Zhang, Yun Yan, and Jianbin Huang*

Beijing National Laboratory for Molecular Sciences (BNLMS), State Key Laboratory for Structural Chemistry of Unstable and Stable Species, College of Chemistry and Molecular Engineering, Peking University, Beijing 100871, China

Received: May 24, 2010; Revised Manuscript Received: July 25, 2010

Supramolecular self-assembly can not only lead to a better understanding of biological systems, but also can enable rational building of complex and functional materials. In this report, hierarchical one-dimensional (1D) architectures involving nanotubes, coiled-coil ropelike structures, nanohelices, and nanoribbons are created via lanthanum−cholate supramolecular self-assembly. These sophisticated self-assemblies are proven to be mediated by temperature. The entanglement of one-dimensional nanostructures is demonstrated to give rise to fascinating "super" hydrogel, which can realize water gelation at extremely low concentration. Unprecedented water gelation behaviors, that is, heating-enhanced stiffness and heating-promoted gelation, are found in lanthanum−cholate supramolecular hydrogel. The driving forces of self-assembled complex nanostructures and the unique role of temperature are also discussed.

Introduction

One-dimensional (1D) nanostructures, such as fiber, belt, helix, and tube, have attracted extensive research interest over the past decade owing to their relevance to biological phenomena[1] and diseases[2] and the beneficial influence of dimensionality on electronic and optical materials.[3] Some interesting examples include cell deformation and division, blood clotting, the DNA double helix, amyloid fibrils, carbon nanotubes, and kinds of 1D semiconductor nanowires. Reliable strategies have been set up to design 1D nanostructures: for instance, vapor deposition,[4] a solution−liquid−solid method,[5] template-directed methods,[6] and molecular self-assembly.[7] Although preferential growth in one dimension has been frequently reported, rational control of the shape and size of 1D nanostructures is less common. Molecular self-assembly held together by relatively weak interactions (e.g., hydrogen bonding, aromatic stacking or metal coordination interactions, etc.), however, provides an easy access to tunable 1D nanostructures rather than covalent connected inorganic material or polymers.

These self-assembled architectures with dynamic nature have been readily built in a controllable fashion and might be easily reconfigured into a variety of morphologies.[8] For example, Oda et al.[9] demonstrate fine-tuning of twisted and helical structures formed from nonchiral dicationic gemini amphiphiles complexed with chiral tartrate anions. The morphologies and dimensions of twisted and helical ribbons, as well as tubules, can be controlled by varying the temperature, introducing small amounts of additives, or slight modification of molecular structure. Stupp[10] has utilized light to remotely realize structural evolution from nanohelix to untwisted nanofibers. Similarly, Shimizu and co-workers[11] have realized reversible photochemical conversion of helicity in self-assembled nanofibers from a thymidylic acid appended bolaamphiphile. Ajayaghosh[12] recently achieved reversible transformation between rings and coils using an oligo(*p*-phenylenevinylene) derivative by dynamic hydrogen-bonding.

One of the appealing advantages of one-dimensional nanostructures is their capability to entangle into a cross-linked network, which can lead to a fascinating soft matter hydrogel.[13] Hydrogels are solidlike materials that can entrap a large portion of water solvent. Owing to the intriguing physicochemical properties, hydrogel can find applications[14] in pollutant capture and removal,[15] sensor arrays,[16] template-directed nanomaterial synthesis,[17] drug delivery,[18] and wound healing[19] and as scaffolds for tissue engineering.[20] From the viewpoint of biorelated applications, low molecular weight hydrogelators are advantageous in their biodegradability and biocompatibility. In addition, "super" hydrogels which are able to realize water gelation at extremely low concentration, are more desirable (usually, the concentration is below 0.1 wt %).[21] Nevertheless, it remains a challenge to create super hydrogels with low molecular weight hydrogelators.

Motivated by versatile functionalities of 1D nanostructure, we present a facile creation toward self-assembled 1D architectures involving nanotubes, coiled-coil ropelike structures, nanohelices, and nanoribbons in a lanthanum−cholate supramolecular system. Subtle control of structural parameters such as morphology, size, and helicity is realized by readily adjusting the temperature. Furthermore the entanglement of 1D nanostructures are found to generate "super" hydrogels, wherein the lowest gelation concentration can be as low as 0.04 wt %. The unique effect of temperature on the supramolecular hydrogel (namely, heating-promoted gelation and heating-enhanced stiffness) is described.

Results and Discussion

Super Hydrogel by Lanthanum−Cholate Supramolecular Self-Assembly. Hydrogel was conveniently obtained by mixing stock solutions of sodium cholate and lanthanum chloride. The

* Corresponding author. Phone: 86-10-62753557. Fax: 86-10-62751708. E-mail: jbhuang@pku.edu.cn.

10.1021/jp1047369
Published on Web 08/19/2010

TABLE 1: Gelation Test of Lanthanum−Cholate Supramolecular System at 25 °C

SC/La^{3+} (mM/mM)	wt %	property[a]	appearance[b]	gel time[c]
0.6/0.6	0.040	G	C	≈10 D
0.9/0.9	0.061	G	T	12−13 h
1.0/1.0	0.06	G	T	11−12 h
1.5/1.5	0.101	G	T	2 min
3.0/3.0	0.202	G	T	<1 min

[a] G: gel, stable to tube inversion. PG: partially gel, unstable to tube inversion. S: solution. [b] C: clear. T: translucent. [c] d: day(s). h: hour(s). min: minute(s).

hydrogelation ability was investigated by an inverted test tube method (Table 1). It is amazing that transparent hydrogel can be obtained at extremely low concentration, ∼0.6 mM sodium cholate and 0.6 mM lanthanum chloride, or 0.04 wt % (Figure S1)! This is to say, one cholate molecule traps around 92 000 water molecules with the assistance of the lanthanum ion. To the best of our knowledge, the lowest gelation concentration of a lanthanum−cholate system is comparable to the most efficient super hydrogelator thus far in the literature.[22] When the lanthanum−cholate concentration was further raised, hydrogelation kinetics can be remarkably promoted, and hydrogel samples became translucent or even opaque in appearance (Table 1).

Dynamic rheology was further performed to investigate the mechanical properties of super hydrogel. Nondestructive frequency sweep in Figure 1a shows lanthanum−cholate hydrogel (1.5 mM/1.5 mM) exhibits typical solidlike rheological behavior with the storage modulus G′ (∼1200 Pa) dominating the loss modulus G″ (∼70 Pa) over the investigated oscillating frequency. Amplitude sweep ($f = 1$ Hz) in Figure 1b indicates weak dependence of G′ and G″ on applied stress until the yield stress (∼8 Pa) is reached. When the gelator concentration is increased, the hydrogel mechanical intensity can be greatly enhanced. For example, the storage modulus G′ and the loss modulus G″ increase to 5000 and 200 Pa, respectively, as the concentration increases to 3.0 mM/3.0 mM in the lanthanum−cholate system. The yield stress of this system is also improved to 90 Pa. This is therefore expected to be a super hydrogel with excellent mechanical performance at low concentration.

Supramolecular Nanostructures in Lanthanum−Cholate Hydrogel. Transmission electronic microscopy (TEM) and field emission-scanning electronic microscopy (FE-SEM) was applied

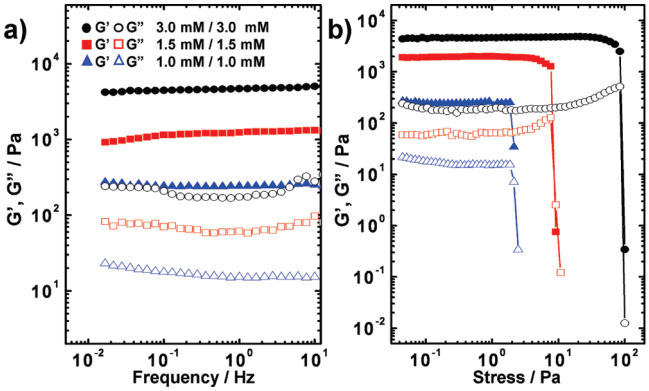

Figure 1. Dynamic rheology of lanthanum−cholate hydrogel: (a) frequency sweep and (b) amplitude sweep of 3 mM/3 mM (black circle), 1.5 mM/1.5 mM (red square), 1.0 mM/1.0 mM (blue triangle). The solid symbols are donated to storage modulus G′, and the open symbols to loss storage G″.

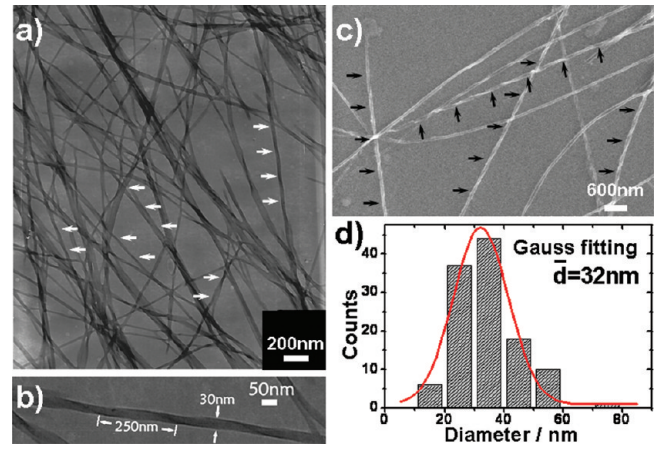

Figure 2. Twisted and untwisted nanoribbons at 25 °C: (a) TEM image, (b) magnified TEM image, and (c) SEM image; and (d) histogram showing the width distribution with an average width of 32 nm.

to reveal the self-assembled nanostructures in super hydrogels. A lanthanum−cholate supramolecular system with a concentration of 1.5 mM/1.5 mM was investigated at 25 °C. As Figure 2a shows, a large amount of one-dimensional twisted nanoribbons with widths ranging from 10 to 80 nm were observed both in TEM and SEM. An enlarged image of TEM indicates the twisted character of one-dimensional nanoribbons with right-handed helicity (Figure 2b). It should be mentioned that the incorporation of lanthanum ions can provide enough contrast toward an electron beam. Consequently, lanthanum−cholate nanotubes can be directly observed under TEM without staining, and artificial structures brought by staining solution can be avoided. The SEM image in Figure 2c also confirms right-handed nanohelices with pitches ranging from 200 to 1000 nm. The length of the twisted ribbons can easily reach to micrometers. Figure 2d gives the statistical distribution of ribbon diameters as collected from TEM images. The Gauss fitting therein demonstrates the mean diameter is 32 nm. Apart from nanohelices, an amount of untwisted nanoribbons with 40−100 nm width are also found at this temperature (Figure 2a). These one-dimensional nanoribbons with a high axial ratio further entangle into a three-dimensional network, which may entrap a large number of water molecules by surface tension or the capillary effect. The imprisoned water within the interstices of the network can impart stability and rigidity to hydrogel systems, which may be responsible for superhydrogel formation.

The Driving Forces of Supramolecular Self-Assemblies. Further experiments were performed to explore the structural origin of lanthanum−cholate self-assembly. Fourier transform infrared (FT-IR) demonstrates the existence of lanthanum−carboxyl coordination in a bidentate chelating fashion (Figure S2 of the Supporting Information), which is believed to contribute to supramolecular self-assembly. The important role of the metal−ligand coordination can be also manifested by replacing La^{3+} with Na^{+} or K^{+}, in which 1D structures and hydrogel cannot be observed. In addition, the addition of EDTA is found to break down the lanthanum−cholate hydrogel, which indicates the indispensable role of lanthanum−carboxyl coordination.

The hydrogen bond between hydroxyl groups of neighboring cholate molecules is also supposed to promote molecular self-assembly. To confirm this hypothesis, we attempted to weaken the intermolecular hydrogen bond by addition of urea into the lanthanum−cholate hydrogel, which is usually considered to be a kind of hydrogen bond competing agent.[23] As expected, one-dimensional nanostructures and hydrogel were destroyed

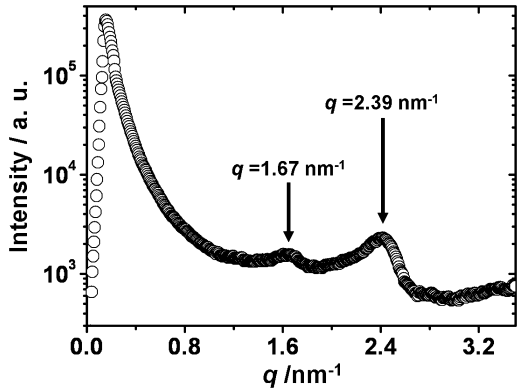

Figure 3. SAXS profile of lanthanum−cholate super hydrogel at 25 °C in situ. The scattering peaks indicate well-ordered packing behavior within organized nanostructures.

with addition of 5 M urea. Moreover, it was found that when sodium cholate was replaced by sodium deoxycholate, which is similar in structure but less hydrophilic, rapid precipitates were generated in the presence of the lanthanum ion. It is therefore proposed that hydrogels can be achieved in a lanthanum−cholate system only with a delicate hydrophilic/hydrophobic balance. Hence, it is believed that the hydrophilic/hydrophobic balance, hydrogen bond, and lanthanum−carboxyl coordination are essential for supramolecular self-assembly in a lanthanum−cholate system.

To encode the superstructure of one-dimensional nanostructures, small-angle X-ray scattering (SAXS) was also conducted. In Figure 3, a strong SAXS peak at $q = 2.39$ nm^{-1} is observed, which corresponds to a d spacing of 26.3 Å and comparable with the duple length of the cholate skeleton (15 Å × 2). As suggested in our previous work,[7a] this scattering peak is attributed to the ordered packing of cholate bilayer units driven by the intermolecular hydrogen bond between cholates.[24] However, the d spacing of 37.6 Å indicated by the reflection peak in the low q region ($q = 1.67$ nm^{-1}) is about 3 times that in the Ca^{2+}−cholate system (~10.6 Å). This suggests the different molecular packing mode between the La^{3+}−cholate and Ca^{2+}−cholate systems.[7a]

Considering the preferred coordinated number of lanthanum is always 7, 8, or 9, one lanthanum ion would coordinate with three carboxyl groups. This is supported by electrospray ionization mass spectra (ESI-MS, Figure S3 of the Supporting Information). Combined with these results, a modified scheme of molecular arrangement is also proposed in Scheme 1. Owing to intermolecular hydrogen bonds, cholate is supposed to arrange into a unique bilayer strips, which approach together via lanthanum−carboxyl coordination (Scheme 1d). In cross-sectional view, two cholate bilayers adapt a nonpolar face-to-nonpolar face arrangement driven by the hydrophobic effect (Scheme 1e). Consequently, a hierarchical lanthanum−cholate supramolecular nanohelix was constructed by the synergic effect of multiple noncovalent interactions. It is worth noting that the hydrophilic surfaces of 1D nanostructures, which are abundant in hydroxyl groups and carboxyl groups, are expected to exhibit great affinity to water molecules and facilitate water gelation at low concentration.

In our previous work, metal-induced one-dimensional nanostructures or hydrogel was reported in sodium cholate solution with the addition of a series of metal ions (such as Ca^{2+}, Ni^{2+}, Zn^{2+}, Co^{2+}, and Cu^{2+}).[7a] However, hydrogelation at extremely low concentration is observed only in a La^{3+}−cholate system. The minimum gelation concentration in Ca^{2+}−, Ni^{2+}−, Zn^{2+}−, Co^{2+}−, and Cu^{2+}−cholate systems is 10 mM/20 mM, 50 mM/50 mM, 2.5 mM/5 mM, 10 mM/20 mM, and 2.5 mM/5 mM, respectively. The superior gelation performance of lanthanum−cholate as compared with other metal−cholate systems

SCHEME 1: Schematic Model of Twisted Nanoribbon[a]

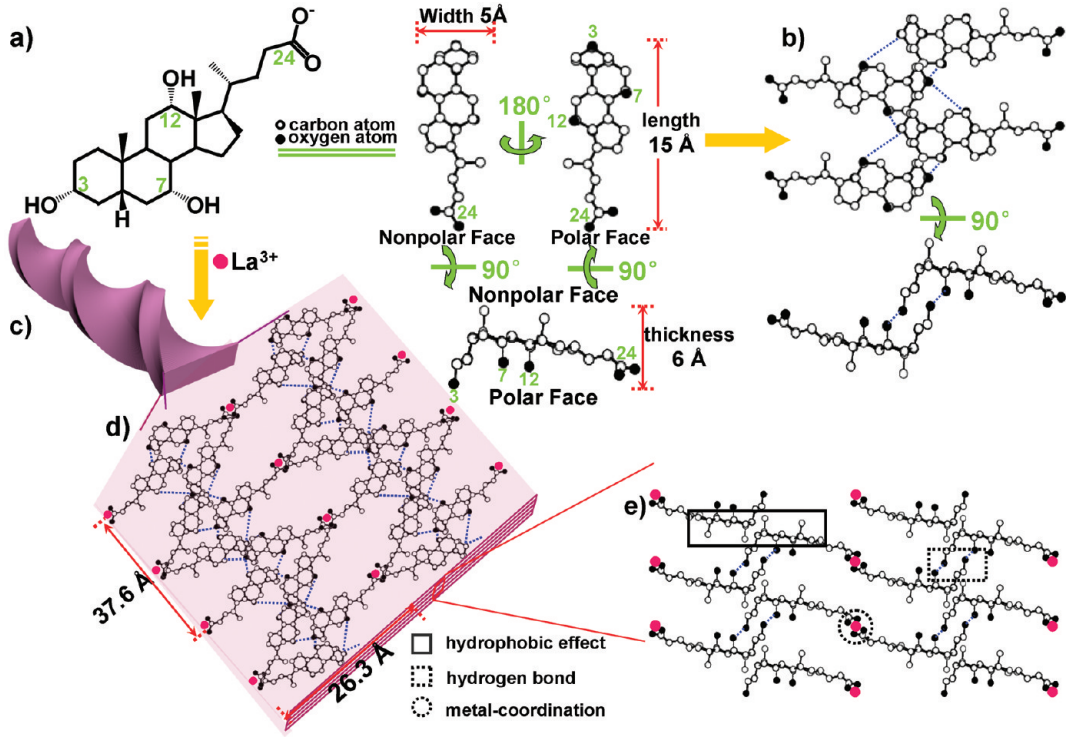

[a] (a) Molecular structure of cholate, (b) molecular aggregate of a bilayer type of cholate host framework (the blue dotted lines denote H-bonds), (c) twisted nanoribbon, (d) top view, and (e) cross-sectional view of the molecular model.

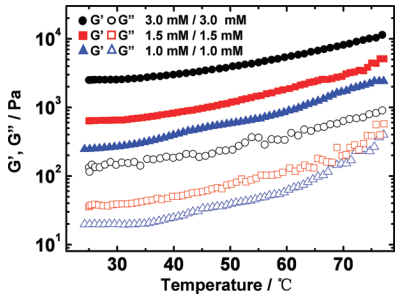

Figure 4. Temperature-sweep oscillation rheology of lanthanum−cholate hydrogel at concentrations of 3 mM/3 mM (black circle), 1.5 mM/1.5 mM (red square), 1.0 mM/1.0 mM (blue triangle) of lanthanum/cholate supramolecular hydrogels. The solid symbols are G′; and the open symbols, G″.

is supposed to stem from the strong lanthanum−cholate interactions. This is because each lanthanum ion possesses three positive charges, which allows its coordination with three cholate molecules effectively. Meanwhile, the multiple charge electrostatic attraction between lanthanum ion and cholate will greatly enhance the lanthanum−cholate affinity. This ultimately promotes the molecular aggregating ability and realizes water gelation at low concentration.

Extraordinary Heating-Promoted Water Gelation. Normally, self-assembled hydrogels may undergo gel−sol phase transition as temperatures increase, accompanied by a reduction in mechanical intensity. The lanthanum−cholate supramolecular hydrogel, however, exhibits strong stability at temperatures as high as 95 °C. To study the temperature effect on water gelation, differential scanning calorimetry (DSC) and dynamic rheology were employed. The DSC heating curve in Figure S4 of the Supporting Information shows no notable endothermic peaks between 5 and 90 °C; in other words, no phase transition occurs. In temperature-sweep oscillation rheology (Figure 4), both the elastic modulus G′ and viscous modulus G″ increase gradually with increasing temperature. As an exemplary system, a lanthanum−cholate hydrogel of 1.5 mM/1.5 mM concentration exhibits a storage modulus, G′, of 700 Pa and loss modulus, G″, of 40 Pa at 25 °C. When the temperature is increased to 50 °C, these two moduli gradually increase to 1400 and 80 Pa, respectively, about 2 times greater than that of 25 °C. Similar results can be found in a lanthanum−cholate hydrogel at different concentrations. Herein, the abnormal phenomenon is described as "heating-enhanced stiffness". On the other hand, the unique temperature effect is also reflected in the gelation kinetics, which is referred to as "heating-promoted gelation". As shown in Table 2, a higher temperature is helpful to speed up the formation of lanthanum−cholate hydrogel. For instance, the lanthanum−cholate hydrogel at a concentration of 0.9 mM/0.9 mM is formed in 12−13 h at 25 °C, but within 4 min at 50 °C.

TABLE 2: Gelation Kinetic of Lanthanum−Cholate System at 4, 15, 25, and 50 °C[a]

SC/La^{3+} (mM/mM)	4 °C	15 °C	25 °C	50 °C
0.6/0.6	S	S	G; 10 d	G; 2 d
1.0/1.0	S	S	G; ≈3 d	G; 2−3 min
1.5/1.5	PG	G; 2−3 d	G; 2 min	G; ≈2 min
3.0/3.0	G; 2−3 d	G; 6 min	G; < 1 min	G; 30 s

[a] Meanings of the symbols are as the same as in Table 1.

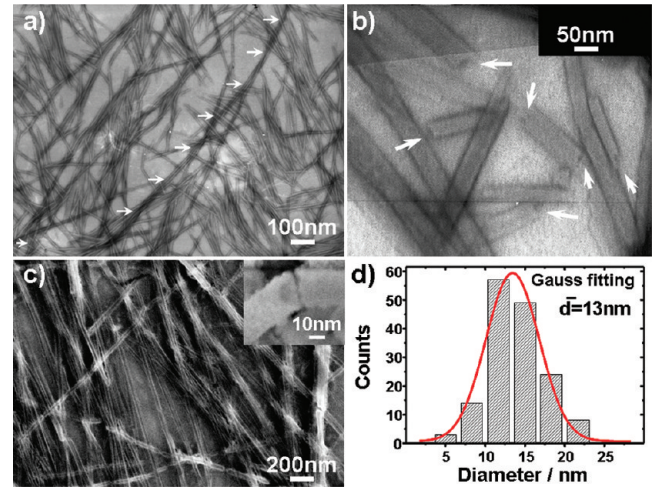

Figure 5. Nanotubes: (a) TEM image; (b) high-magnification of the nanotubes showing the open end; (c) SEM image showing the hollow feature; (d) histogram of diameter distribution (T = 4 °C).

Temperature-Dependent Supramolecular Nanostructures. The extraordinary temperature-dependent hydrogelation is supposed to originate from self-assembled structure at nanoscale, which was systematically studied at 4, 15, and 50 °C. When the sample was equilibrated at 4 °C, uniform nanotubes with 5−25 nm diameter were observed under TEM (Figure 5a). The nanotubes can extend to several micrometers in length, as designated by the arrows. The differences in contrast between the edge and middle of the same tube stem from mass−thickness contrast owing to the tubular hollow feature. An enlarged image of the nanotubes is presented in Figure 5b, in which the arrows point to the elliptical open end of hollow tubes. It is found that the wall thickness of the nanotubes is only about 2−3 nm. FE-SEM operated at a relatively high accelerated voltage of 5 kV (for an organic sample) reveals the internal hollow structure of nanotubes by different contrast (Figure 5c) and agrees well with TEM results. The insert clearly shows the open end of the tube. Figure 5d shows the statistical distribution of the tube diameters as collected from TEM images. The Gauss fitting therein shows that the mean diameter of the nanotubes is 13 nm, which is slightly smaller than that at 25 °C.

When the sample was incubated at 15 °C, the number of tubular structures was greatly reduced, and typical right-handed nanohelices became the dominating morphology (Figure 6a−c). The helices exhibit the twisted shape of the nanoribbons with ∼90−400 nm pitches and a thickness of several nanometer. The nanoribbon lengths can extent to several micrometers, and the width ranges from 10 to 60 nm, slightly larger than that of nanotubes at 4 °C. It is interesting to find that the twisted pitches can increase with the increase in the nanoribbon width. The width distribution analysis with Gauss fitting reveals an average diameter of ∼25 nm (Figure 6d). In this sample, the braided patterns originating from 2D projection of two intertwining coils of nanoribbons can also be seen, as pointed out by arrows in Figure 6e. FE-SEM images also prove the existence of the superhelical coiled-coil, ropelike nanostructures with right-handed bias (Figure 6f). It is also noted in Figure 6g that there are some pseudoropelike structures with a helical ribbon twining round a straight ribbon.

Finally as the sample temperature increased to 50 °C, helical nanoribbons were no longer observable under SEM and TEM (Figure 7a, b). Instead, one-dimensional untwisted nanoribbons were the exclusive self-assembled structures. The nanoribbons' widths range from 30 to 150 nm, and the length can reach to

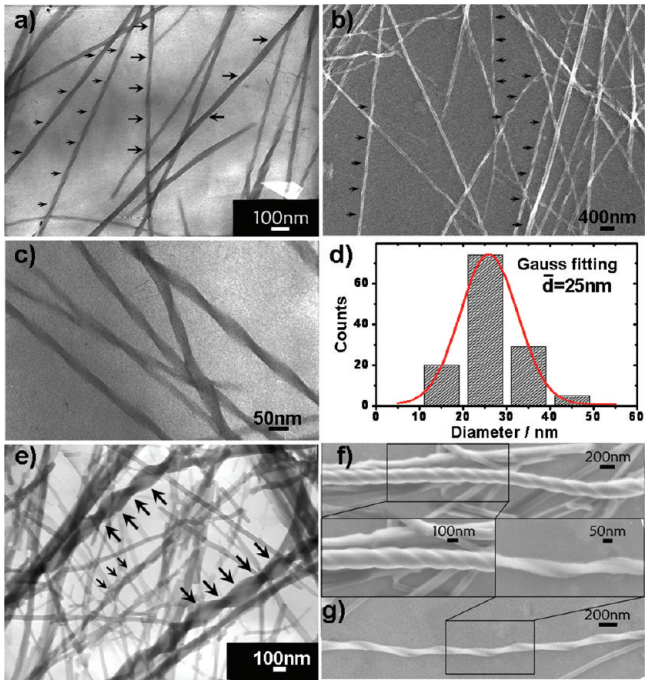

Figure 6. Twisted nanoribbons: (a, c) TEM, (b) SEM image, and (d) histogram of width distribution. Coiled-coil rope-like structure: (e) TEM and (f, g) SEM (T = 15 °C).

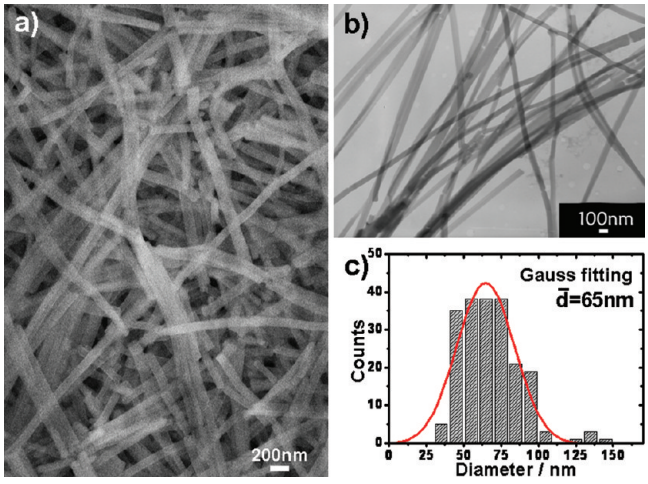

Figure 7. Nanoribbons in lanthanum−cholate supramolecular system: (a) SEM, (b) TEM images, and (c) width distribution histogram (T = 50 °C).

several micrometers. Gauss fitting of the nanoribbons' diameter distribution reveals an average diameter of 65 nm, which is obviously larger than that at low temperatures (Figure 7c).

Temperature Effect on Hierarchical Nanostructures and Super Hydrogel. On the basis of the results of TEM and SEM, it appears that a lanthanum−cholate supramolecular system experiences an evolutionary development from nanotubes to coiled-coil helical ropes; twisted nanoribbons; and finally, to nanoribbons as the temperature increases (Scheme 2). Continuous growth in the size of the self-assembled nanostructures was also found with increasing temperature. The unique temperature effect was supposed to arise from hydroxyl groups of cholate molecules. As Scheme 1 shows, the hydroxyl groups of cholate molecules can interact with water via hydrogen bond, which contributes to cholate hydrophilicity. When the temperature is raised, the hydrogen bonds between water and cholate are weakened, leading to lower hydrophilicity. This is believed to

SCHEME 2: Representative Scheme of Temperature-Dependent Nanostrucutural Evoluation of the Hydrogel

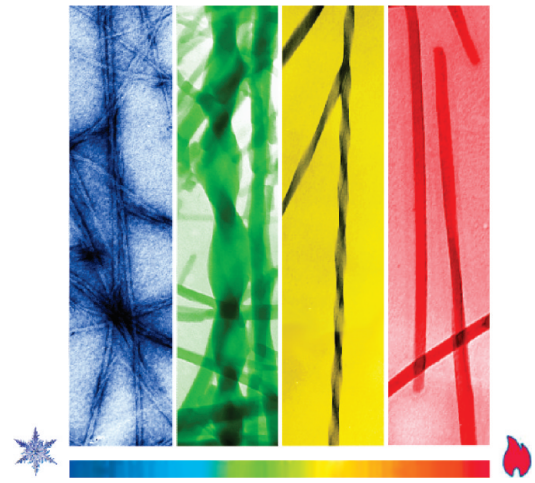

be the structural origin of temperature-dependent lanthanum−cholate self-assembly. Benefiting from a decrease in hydrophilicity, lanthanum−cholate's aggregating ability is promoted, and larger aggregates can be formed at higher temperatures.

It can be also noted that highly curved structures, such as a twisted nanohelix and nanotubes, are formed at low temperature, whereas nontwisted ribbons exist at higher temperatures. This is because high-curvature nanotubes and twisted nanoribbons are closely related to lower values of bending rigidity, which depends on the sample temperature in the lanthanum−cholate system. As stated above, the aggregating ability of lanthanum−cholate is enhanced at higher temperatures, which results in self-assembled a 1D nanostructure with a larger diameter and close packing of building units. Both factors can lead to higher bending rigidity of self-assembled nanostructures. Therefore, highly curved nanostructures are not favored at high temperatures, and it should be possible to fabricate nanotubes and twisted ribbons only at lower temperatures.

The temperature-dependent supramolecular nanostructure at nanometer scale can ultimately impart great influence to self-assembled hydrogel at the macroscopic scale. First, the heating-driven size growth of nanotubes, nanoribbons, and nanobelts may strengthen the mechanical stability of 1D nanostructures as well as cross-linked 3D networks, which ultimately enhances the hydrogel mechanical intensity as revealed by rheology. Meanwhile, water gelation kinetics is also accelerated by the enhancement of molecular hydrophobicity with increasing temperature.

Conclusion

In conclusion, temperature-controlled, one-dimensional hierarchical architectures including nanotubes; coiled-coil, rope-like structures; nanohelices; and nanoribbons were fabricated by supramolecular self-assembly. A fascinating super hydrogel arising from the entanglement of one-dimensional nanostructures was obtained. These supramolecualr hydrogels display unprecedented "heating-enhanced stiffness" and "heating-promoted gelation" behavior. Multiple weak molecular interactions, such as hydrophobic effect, metal−ligand cooperation, and hydrogen bonds, are supposed to account for supramolecular self-assemblies in the lanthanum−cholate system. The superstruc-

tures of complex nanostructures were provided with the combined result of SAXS, FT-IR, and ESI-MS. The temperature-mediated hydrogen bonds between water and cholate are believed to be the structural origin of temperature-dependent lanthanum−cholate self-assembly. We hope this work can give some insights into the self-assembled, one-dimensional nanostructures with controllable shape and size, as well as super hydrogel formed by low molecular weight gelators. It is also anticipated that lanthanum−cholate hydrogel can find versatile applications in cell culture, tissue engineering, and materials science.

Acknowledgment. This work was supported by the National Natural Science Foundation of China (20873001, 20633010 and 50821061) and National Basic Research Program of China (Grant no. 2007CB936201).

Supporting Information Available: Experimental procedures; the macroscopic appearance of the hydrogel; IR, ESI-MS spectra; and DSC curve of the lanthanum−cholate supramolecular system are available as Supporting Information. This material is available free of charge via the Internet at http://pubs.acs.org.

References and Notes

(1) Scheibel, T. *Curr. Opin. Biotechnol.* **2005**, *16*, 427.

(2) (a) Binder, W. H.; Smrzka, O. W. *Angew. Chem., Int. Ed.* **2006**, *118*, 7324. (b) Ross, C. A.; Poirier, M. A. *Nat. Med.* **2004**, S10. (c) Makin, O. S.; Atkins, E.; Sikorski, P.; Johansson, J.; Serpell, L. C. *Proc. Natl. Acad. Sci. U.S.A.* **2005**, *102*, 315. (d) Guo, J.-P.; Arai, T.; Miklossy, J.; McGeer, P. L. *Proc. Natl. Acad. Sci. U.S.A.* **2006**, *103*, 1953.

(3) Xia, Y. N.; Yang, P. D.; Sun, Y. G.; Wu, Y. Y.; Mayers, B.; Gates, B.; Yin, Y. D.; Kim, F.; Yan, Y. Q. *Adv. Mater.* **2003**, *15*, 353.

(4) (a) Duan, X. F.; Huang, Y.; Cui, Y.; Wang, J. F.; Lieber, C. M. *Nature* **2001**, *409*, 66. (b) Alivisatos, A. P. *Science* **1996**, *271*, 933.

(5) (a) Holmes, J. D.; Johnston, K. P.; Doty, R. C.; Korgel, B. A. *Science* **2000**, *287*, 1471. (b) Trentler, T. J.; Hickman, K. M.; Geol, S. C.; Viano, A. M.; Gibbons, P. C.; Buhro, W. E. *Science* **1995**, *270*, 1791.

(6) (a) Ogihara, H.; Sadakane, M.; Nodasaka, Y.; Ueda, W. *Chem. Mater.* **2006**, *18*, 4981. (b) Jung, J. H.; Kobayashi, H.; van Bommel, K. J. C.; Shinkai, S.; Shimizu, T. *Chem. Mater.* **2002**, *14*, 1445. (c) Kobayashi, S.; Hamasaki, N.; Suzuki, M.; Kimura, M.; Shirai, H.; Hanabusa, K. *J. Am. Chem. Soc.* **2002**, *124*, 6550. (d) Sone, E. D.; Zubarev, E. R.; Stupp, S. I. *Angew. Chem., Int. Ed.* **2002**, *41*, 1706. (e) Seddon, A. M.; Patel, H. M.; Burkett, S. L.; Mann, S. *Angew. Chem., Int. Ed.* **2002**, *41*, 2988. (f) Yuwono, V. M.; Hartgerink, J. D. *Langmuir* **2007**, *23*, 5033.

(7) (a) Qiao, Y.; Lin, Y. Y.; Wang, Y. J.; Yang, Z. Y.; Liu, J.; Zhou, J.; Yan, Y.; Huang, J. B. *Nano Lett.* **2009**, *9*, 4500. (b) Bae, J.; Choi, J.-H.; Yoo, Y.-S.; Oh, N.-K.; Kim, B.-S.; Lee, M. *J. Am. Chem. Soc.* **2005**, *127*, 9668. (c) Cui, H. G.; Chen, Z. Y.; Zhong, S.; Wooley, K. L.; Pochan, D. J. *Science* **2007**, *317*, 647. (d) Lin, Y. Y.; Wang, A. D.; Qiao, Y.; Gao, C.; Drechsler, M.; Ye, J. P.; Yan, Y.; Huang, J. B. *Soft Matter* **2010**, *6*, 2031. (e) Ajayaghosh, A.; Varghese, R.; George, S. J.; Vijayakumar, C. *Angew. Chem., Int. Ed.* **2006**, *45*, 1141. (f) Jung, J. H.; Kobayashi, H.; Masuda, M.; Shimizu, T.; Shinkai, S. *J. Am. Chem. Soc.* **2001**, *123*, 878. (g) Jin, W. S.; Fukushima, T.; Niki, M.; Kosaka, A.; Ishii, N.; Aida, T. *Proc. Natl. Acad. Sci. U.S.A.* **2005**, *102*, 10801. (h) Bhattacharya, S.; Pal, A. *J. Phys. Chem. B* **2008**, *112*, 4918. (i) Li, Y. G.; Liu, K. Q.; Liu, J.; Peng, J. X.; Feng, X. L.; Fang, Y. *Langmuir* **2006**, *22*, 7016. (j) Zhai, L. M.; Herzog, B.; Drechsler, M.; Hoffmann, H. *J. Phys. Chem. B* **2006**, *110*, 17697. (k) Ghosh, A.; Dey, J. *J. Phys. Chem. B* **2008**, *112*, 6629.

(8) (a) Lehn, J.-M. *Rep. Prog. Phys.* **2004**, *67*, 249. (b) Kiyonaka, S.; Sugiyasu, K.; Shinkai, S.; Hamachi, I. *J. Am. Chem. Soc.* **2002**, *124*, 10954. (c) Ketner, A. M.; Kumar, R.; Davies, T. S.; Elder, P. W.; Raghavan, S. R. *J. Am. Chem. Soc.* **2007**, *129*, 1553. (d) Lin, Y. Y.; Qiao, Y.; Yan, Y.; Huang, J. B. *Soft Matter* **2009**, *5*, 3047. (e) Gräbner, D.; Zhai, L.; Talmon, Y.; Schmidt, J.; Freiberger, N.; Glatter, O.; Herzog, B.; Hoffmann, H. *J. Phys. Chem. B* **2008**, *112*, 2901.

(9) (a) Oda, R.; Huc, I.; Candau, S. J. *Angew. Chem., Int. Ed.* **1998**, *37*, 2689. (b) Brizard, A.; Aimé, C.; Labrot, T.; Huc, I.; Berthier, D.; Artzner, F.; Desbat, B.; Oda, R. *J. Am. Chem. Soc.* **2007**, *129*, 3754.

(10) Muraoka, T.; Cui, H. G.; Stupp, S. I. *J. Am. Chem. Soc.* **2008**, *130*, 2946.

(11) Iwaura, R.; Shimizu, T. *Angew. Chem., Int. Ed.* **2006**, *45*, 4601.

(12) Yagai, S.; Kubota, S.; Saito, H.; Unoike, K.; Karatsu, T.; Kitamura, A.; Ajayaghosh, A.; Kanesato, M.; Kikkawa, Y. *J. Am. Chem. Soc.* **2009**, *131*, 5408.

(13) For recent reviews, see: (a) Estroff, L. A.; Hamilton, A. D. *Chem. Rev.* **2004**, *104*, 1201. (b) Sangeetha, N. M.; Maitra, U. *Chem. Soc. Rev.* **2005**, *34*, 821. (c) de Loos, M.; Feringa, B. L.; van Esch, J. H. *Eur. J. Org. Chem.* **2005**, 3615. (d) Trickett, K.; Eastoe, J. *Adv. Colloid Interface Sci.* **2008**, *144*, 66. (e) Raghavan, S. R. *Langmuir* **2009**, *25*, 8382. For papers, see: (f) Suzuki, M.; Yumoto, M.; Kimura, M.; Shirai, H.; Hanabusa, K. *Chem. Commun.* **2002**, 884. (g) Maitra, U.; Mukhopadhyay, S.; Sarkar, A.; Rao, P.; Indi, S. S. *Angew. Chem., Int. Ed.* **2001**, *40*, 2281. (h) Iwaura, R.; Yoshida, K.; Masuda, M.; Yase, K.; Shimizu, T. *Chem. Mater.* **2002**, *14*, 3047. (i) Haines, S. R.; Harrison, R. G. *Chem. Commun.* **2002**, 2846. (j) Frkanec, L.; Jokic, M.; Makarevic, J.; Wolsperger, K.; Zinic, M. *J. Am. Chem. Soc.* **2002**, *124*, 9716. (k) Schneider, J. P.; Pochan, D. J.; Ozbas, B.; Rajagopal, K.; Pakstis, L.; Kretsinger, J. *J. Am. Chem. Soc.* **2002**, *124*, 15030. (l) Ghosh, A.; Dey, J. *Langmuir* **2009**, *25*, 8466. (m) Maiti, R.; Dey, J. *Chem. Commun.* **2006**, 4903. (n) Morán, M. C.; Miguel, M. G.; Lindman, B. *Langmuir* **2007**, *23*, 6478.

(14) Weiss, R. G., Terech, P., Eds.; *Molecular Gels: Materials with Self Assembled Fibrillar Network*; Spinger: Dordrecht, 2006.

(15) Esser-Kahn, A. P.; Iavarone, A. T.; Francis, M. B. *J. Am. Chem. Soc.* **2008**, *130*, 15820.

(16) (a) Yang, Z.; Xu, B. *Chem. Commun.* **2004**, 2424. (b) Kiyonaka, S.; Sada, K.; Yoshimura, I.; Shinkai, S.; Kato, N.; Hamachi, I. *Nat. Mater.* **2004**, *3*, 58. (c) Koshi, Y.; Nakata, H.; Yamane, E.; Hamachi, I. *J. Am. Chem. Soc.* **2006**, *128*, 10413.

(17) (a) Love, C. S.; Chechik, V.; Smith, D. K.; Wilson, K.; Ashworth, I.; Brennan, C. *Chem. Commun.* **2005**, 1971. (b) Hartgerink, J. D.; Beniash, E.; Stupp, S. I. *Science* **2001**, *294*, 1684. (c) Liu, G.; Zhao, D. C.; Tomsia, A. P.; Minor, A. M.; Song, X. Y.; Saiz, E. *J. Am. Chem. Soc.* **2009**, *131*, 9937.

(18) (a) Zhao, F.; Ma, M. L.; Xu, B. *Chem. Soc. Rev.* **2009**, *38*, 883. (b) Friggeri, A.; Feringa, B. L.; van Esch, J. *J. Controlled Release* **2004**, *97*, 241. (c) Tiller, J. C. *Angew. Chem., Int. Ed.* **2003**, *42*, 3072. (d) Vemula, P. K.; Li, J.; John, G. *J. Am. Chem. Soc.* **2006**, *128*, 8932.

(19) (a) Yang, Z. M.; Liang, G. L.; Guo, Z. F.; Guo, Z. H.; Xu, B. *Angew. Chem., Int. Ed.* **2007**, *46*, 8216. (b) Ellis-Behnke, R. G.; Liang, Y. X.; You, S. W.; Tay, D. K. C.; Zhang, S. G.; So, K. F.; Schneider, G. E. *Proc. Natl. Acad. Sci. U.S.A.* **2006**, *103*, 5054.

(20) Lee, K. Y.; Mooney, D. J. *Chem. Rev.* **2001**, *101*, 1869.

(21) (a) Liu, J.; He, P. L.; Yan, J. L.; Fang, X. H.; Peng, J. X.; Liu, K. Q.; Fang, Y. *Adv. Mater.* **2008**, *20*, 2508. (b) Nagasawa, J.; Kudo, M.; Hayashi, S.; Tamaoki, N. *Langmuir* **2004**, *20*, 7907. (c) Zinic, M.; Vogtle, F.; Fages, F. *Top. Curr. Chem.* **2005**, *256*, 39. (d) Tu, T.; Assenmacher, W.; Peterlik, H.; Weisbarth, R.; Nieger, M.; Dotz, K. H. *Angew. Chem., Int. Ed.* **2007**, *46*, 6368.

(22) (a) van Bommel, K. J. C.; van der Pol, C.; Muizebelt, I.; Friggeri, A.; Heeres, A.; Meetsma, A.; Feringa, B. L.; van Esch, J. *Angew. Chem., Int. Ed.* **2004**, *43*, 1663. (b) Kobayashi, H.; Friggeri, A.; Koumoto, K.; Amaike, M.; Shinkai, S.; Reinhoudt, D. N. *Org. Lett.* **2002**, *4*, 1423.

(23) Mirsky, A. E.; Pauling, L. *Proc. Natl. Acad. Sci. U.S.A.* **1936**, *22*, 439.

(24) (a) Lindman, B.; Kamenka, N.; Fabre, H.; Uimius, J.; Wieloch, T. *J. Colloid Interface Sci.* **1980**, *73*, 556. (b) Zana, R.; Guveli, D. *J. Phys. Chem.* **1985**, *89*, 1687.

JP1047369